# CHAPTER V
# ETHANOL TRANSFORMATION DURING CATALYTIC DEHYDRATION OF BIO-ETHANOL USING COBALT CATALYSTS: EFFECT OF DIFFERENT OXIDATION STATES

## 5.1 Abstract

The catalytic dehydration of bio-ethanol is one of the most attractive routes for producing high cost oxygenate compounds and hydrocarbons in the gasoline range. In this work, 5 wt% Co-promoted alumina, which was prepared by using incipient wetness impregnation method, was used to examine the formation of oxygenates and hydrocarbons in the catalytic dehydration of bio-ethanol. A 3 g of catalyst was examined in the continuous fixed bed U-tube reactor at 500°C under the controlled pressure with 0.5 $h^{-1}$ LHSV of bio-ethanol. The catalyst was characterized using SAA, XRD, and XPS. Moreover, the products were analyzed using GC-online and GC×GC-TOF/MS in order to identify the gaseous products and hydrocarbon species, respectively. As a result, it was found that different oxidation states of cobalt promoter promoted different pathways of ethanol transformation. Compared to parent $Al_2O_3$, $Co/Al_2O_3$ favored to promote ethanol dehydration, leading to the increases in hydrocarbons, and benzene was found as a main hydrocarbon product. However, $Co_3O_4/Al_2O_3$ favored to promote ethanol dehydrogenation, resulting in the increasing of oxygenate compounds. Moreover, the oxygenate compounds were composed of phenol and ketone compounds as main components. Furthermore, XPS analysis indicated that metallic Co was partially transform to CoO after the catalytic testing.

## 5.2 Introduction

The catalytic dehydration of bio-ethanol has been one of the most attractive processes for alternatively producing chemicals, since it has advantages such as low production cost, low energy consumption, low $CO_2$ emission, greener, environmental friendly, especially no waste and toxic compound generation (Takahara *et al.*, 2007).

Generally, the product obtained from ethanol dehydration consists of two main parts; that are, oxygenates and hydrocarbons. Therefore, the transformation of ethanol can take place via two competitive pathways. The first pathway involves the formation of oxygenates, such as ethers, aldehydes, and ketones, via ethanol dehydrogenation. Many kinds of oxygenate compounds can be used as an additive in petroleum oil. For examples, Methyl-Tertiary-Butyl-Ether (MTBE) is used as octane booster to increase octane number, resulting in more complete combustion. However, oxygenate compounds are not only used as an additive in petroleum oil, but also as a solvent in many applications. For example, 2-pentanone is an important solvent for dewaxing process, and also used as a cleaning agent in medical treatment. 3-pentanone is used as a solvent in painting, and as a precursor for producing vitamin E in pharmaceutical industries. The second pathway of ethanol dehydration involves the formation of hydrocarbons, mostly ranging from $C_1$ – $C_{10}$. At present, zeolites are the most popular group of solid acid catalysts employed in the catalytic dehydration of ethanol. Researchers discovered that zeolite catalysts were better than solid oxide catalysts due to the requirement of a lower reaction temperature. These zeolites include HZSM-5, H-mordernite, H-Beta and HY. Among these zeolite catalysts, HZSM-5 is the most popular one used for the catalytic dehydration of ethanol, but it has some disadvantages because there is a large amount of aromatic hydrocarbons in the product mixtures.

In order to avoid aromatics formation, $\gamma$-$Al_2O_3$ is one of alternative catalysts for the catalytic dehydration of ethanol to produce ethylene without containing aromatics due to it has low acidity and large pore sizes. Many research works related to ethylene production by using $\gamma$-$Al_2O_3$ were published, but the reaction required a high reaction temperature (450°C) and offered low ethylene yield (80%). Kagyrmanova *et al.*, (2011) studied the kinetic model of bio-ethanol conversion to ethylene over an alumina-based catalyst. Their experiment was set up at atmospheric pressure, the reaction temperatures in the range of 350-450°C, and the majority of obtained products were ethylene, diethyl ether and butylene. Moreover, Zhang *et al.*, (2008) found that using $\gamma$-alumina at 450°C, the product consisted of 78.7% ethylene, 14.4% ethanol, 6.9% diethyl ether, and 0.1% acetaldehyde.In the last decade, cobalt catalysts were widely employed, aiming to produce hydrocarbons. Bechara *et al.*,

(2001) studied cobalt-supported alumina for producing hydrocarbons in Fischer-Tropsch synthesis. The results showed that the catalyst were selective to produce hydrocarbons in the range of gasoline to waxes. Iglesia (1997) mentioned that $C_{5+}$ selectivity increased with increased cobalt site density because the re-adsorption of $\alpha$-olefins led to initiation of alkyl surface chains and then large hydrocarbon formation. Cant *et al.*, (2013) studied ethylene oligomerization using cobalt-supported silica catalysts. They found that the catalysts were selective to produce hydrocarbons in the range of $C_4$ to $C_6$. On the contrary, cobalt oxide catalysts can be used to produce oxygenate compounds, like aldehyde via methanol dehydrogenation or oxidation. Ozkan *et al.*, (1990) studied first-row transition metal oxide catalysts that contained Cr, Mn, Fe, Co, Ni, and Cu in methanol oxidation. They found that all catalysts can drive the reaction, and exhibited similar behavior in methanol oxidation. Likewise, in 2010, Zafeiratose and co-worker studied cobalt catalysts for producing aldehyde in methanol oxidation. The results showed that the catalysts can stimulate the reaction, and yield aldehyde as a product. In addition, $\gamma$-$Al_2O_3$ is classified as one kind of acid catalysts which has low acidity and large pore size. Therefore, $\gamma$-$Al_2O_3$ might be a proper support to promote large molecules from the catalytic dehydration of bio-ethanol. Moreover, it has been found that the change of oxidation state of a metal catalyst governed the selectivity of the product obtained from the catalytic dehydration of bio-ethanol. Recently, Chinniyomphanich and Jitkarnka (2014), investigated the effect of oxidation state of tin catalysts in the catalytic dehydration of bio-ethanol. The results showed that different oxidation states were affected to different product distributions.

Therefore, in this work, cobalt catalysts of both metal and metal oxide on alumina support were in investigated, aiming to examine the product distribution obtained from the catalytic dehydration of bio-ethanol. Moreover, since the oxidation state of a metal catalyst might change because of the oxidizing conditions of ethanol dehydration, the effect of different oxidation states of Co on th selectivity of products was also investigated. Additionally, cobalt-modified catalysts were characterized using surface area analyzer (SAA), X-ray diffraction spectroscopy (XRD), and X-ray photoelectron spectroscopy (XPS).

## 5.3 Experimental

### 5.3.1 Catalyst Preparation

$\gamma$-$Al_2O_3$ ($\gamma$-Alumina) used in this work was supplied form Sigma Aldrich, Singapore. Cobalt (II) nitrate hexahydrate was used as the cobalt precursor. A solution of cobalt nitrate was loaded on the support using incipient wetness impregnation technique until the amount of 5.0 wt% Co loading was achieved. After impregnation, the wet catalyst was dried at 110°C overnight, and then calcined, starting from room temperature 600°C with the rate of 10°C/min, and held for 3 hours. After that the calcined catalyst was pelletized, crushed, and sieved to 20-40 mesh particles. Additionally, to produce $Co/Al_2O_3$, the calcined catalyst was pretreated with $H_2$ at 650°C for 4 hours.

### 5.3.2 Catalytic Dehydration of Bio-ethanol

The catalytic dehydration of bio-ethanol was performed in a continuous isothermal fixed-bed U-tube reactor controlled at 500°C under atmospheric pressure for 8 hours. The high purity grade bio-ethanol (99.5%) was fed by a syringe pump with carrier gas, helium, through the catalyst bed. The gaseous product was passed through an online-GC, and the liquid condensed in a cooling unit was collected, and after 8 hour time-on-stream, the oil was extracted from the liquid product by using carbon disulfide.

### 5.3.3 Product Analysis

The gaseous products were analyzed by using a GC-TCD (Agilent 6890N) to determine the gas composition, and GC-FID (Agilent 6890N) was used to determine the bio-ethanol and oxygenate contents. The extracted oils were analyzed by using Gas Chromatography (Agilent technology 7890) with Time-of-Fight Mass Spectrometer (LECO, Pegasus® 4D TOF/MS) equipped with the 1$^{st}$ GC column was a non-polar Rtx®-5sil MS (30 m × 0.25 mm × 0.25 μm), and the 2$^{nd}$ GC column was an Rxi®-17 MS column (1.790 m × 0.1 mm ID ×0.1 μm) to determine the composition.

5.3.4 Catalyst Characterization

The Brunauer-Emmett-Teller (BET) technique was used to determine the specific surface area, total pore volume, and pore size of catalysts using Thermo Finnigan/Sorptomatic 1990 surface area analyzer. The pore size distribution was calculated using BJH method. The X-ray diffraction of catalysts was determined using RigaguSmartLab® in BB/Dtex mode with CuK$\alpha$ radiation. The machine collected the data from 10°-80° (2$\theta$) at 5°/min with the increment of 0.01°. X-ray Photoelectron Spectroscopy (XPS) spectra were carried out using a AXIS ULTRA$^{DLD}$. The system was equipped with a monochromatic Al X-ray source and hemispherical analyzer. The spectrometer was operated with the pass energy of 160 and 40 eV for wide and narrow scan, respectively. All peaks were calibrated from referring C 1s spectra located at 284.8 eV

## 5.4 Results and Discussion

5.4.1 Catalyst Characterization

The XRD patterns of catalysts are shown in Figure 5.1. It can be noticed that the peak of $\gamma$-alumina can be detected at 2$\theta$ =67.5° (Liu *et al.*, 2012). Moreover, the XRD patterns of the calcined and reduced catalysts are shown in Figure 5.1 (B) and (C), respectively. The peaks due to $Co_3O_4$ are detected at 2$\theta$ = 31.37°, 45.41°, 59.37° and 65.22° (Batista *et al.*, 2003), and the peak due to metallic Co is detected at 2$\theta$ = 44.3° (Wang *et al.*, 2012). Additionally, the peak that represents the characteristics of $\gamma$-alumina still appear at 2$\theta$ = 67.3° in both samples. These mean that $Co_3O_4$ is formed on the surface of the alumina catalyst, and metallic Co is present in the surface of the reduced catalyst. Therefore, the preparations of $Co_3O_4/Al_2O_3$ and $Co/Al_2O_3$ catalysts were proven successful.

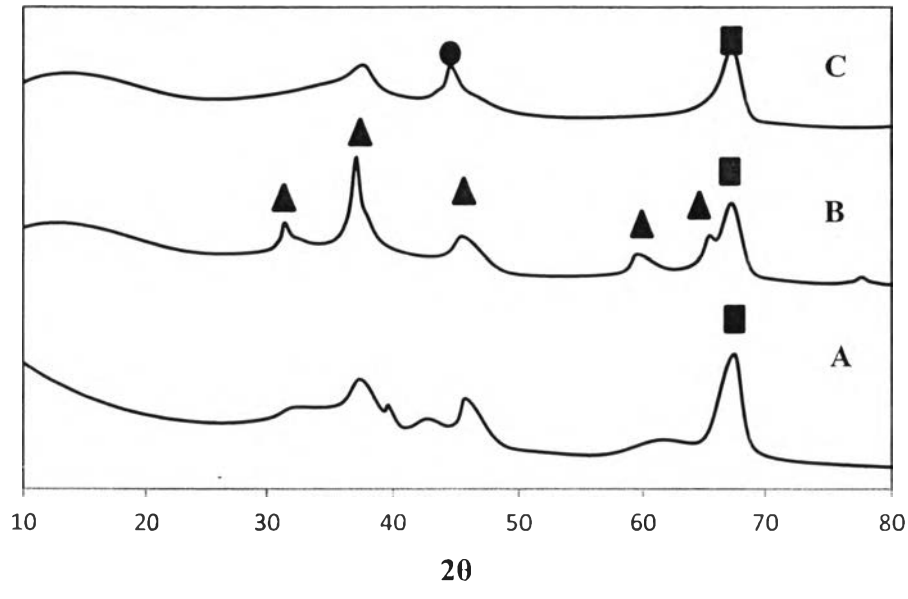


**Figure 5.1** XRD patterns of (A) $Al_2O_3$, (B) $Co_3O_4/Al_2O_3$, and (C) $Co/Al_2O_3$ ( ■ = $Al_2O_3$, ● = Co, and ▲ = $Co_3O_4$).

**Table 5.1** Binding energies of cobalt on fresh and spent catalysts

| Sample | | Co $2p_{3/2}$ | | Co $2p_{3/2}$ (sat.) | | % Composition | |
|---|---|---|---|---|---|---|---|
| | | Fresh | Spent | Fresh | Spent | Fresh | Spent |
| $Co/Al_2O_3$ | Co | 778.6 | 777.1 | - | - | 93.9 | 3.6 |
| | CoO | 781.6 | 781.4 | 785.2 | 785.9 | 6.1 | 96.4 |
| $Co_3O_4/Al_2O_3$ | CoO | 781.5 | 781.9 | 786.5 | 786.9,790.9 | 30.8 | 100 |
| | $Co_3O_4$ | 779.4 | - | - | | 69.2 | - |

Sat.= Shake up satellite

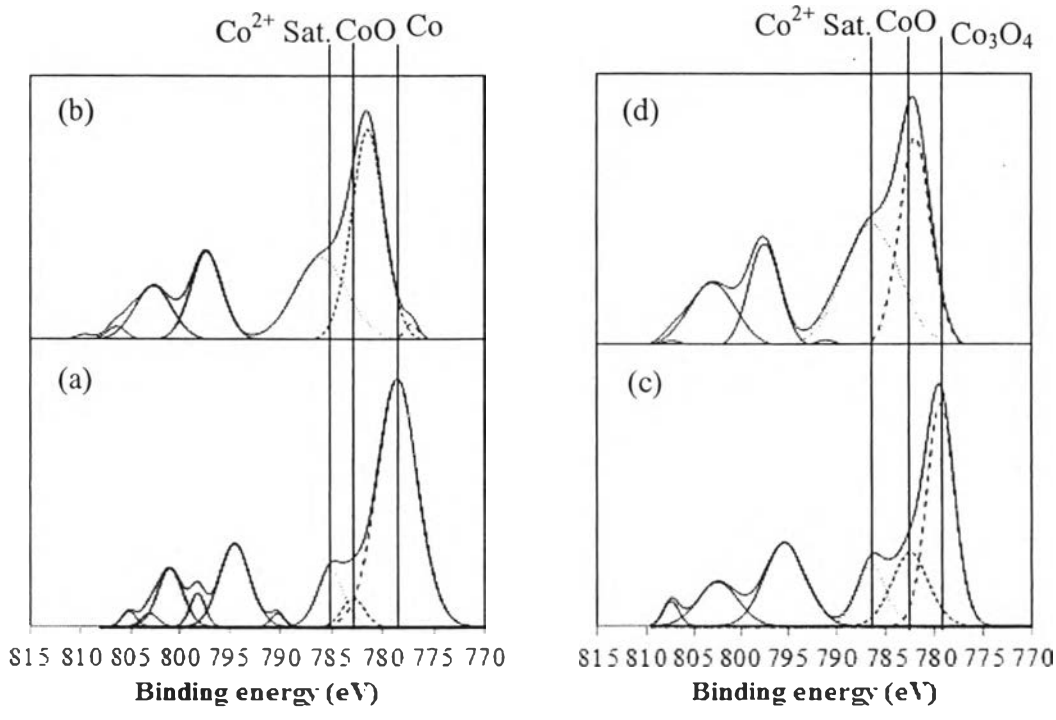


**Figure 5.2** XPS spectra of (a) fresh $Co/Al_2O_3$, (b) spent $Co/Al_2O_3$, (c) fresh $Co_3O_4/Al_2O_3$, and (d) spent $Co_3O_4/Al_2O_3$.

To further verify the chemical state of cobalt on the surface of both samples. X-ray Photoelectron Spectroscopy was employed, and the results are shown in Figure 5.2 and Table 5.2. Figure 5.2 (a) displays the XPS spectra of $Co/Al_2O_3$ catalyst. The $Co2p_{3/2}$ binding energies located at 778.6 and 781.6 eV are assigned to $Co^{(0)}$ (Biesinger *et al.*, 2012) and CoO (Khassin *et al.*, 2012), respectively. Moreover, the characteristic satellite of $Co^{2+}$ is observed at 785.2 eV (Khassin *et al.*, 2012). For the spent $Co/Al_2O_3$ catalyst, Figure 5.2 (b) exhibits that the Co $2p_{3/2}$ binding energies at 777.1 and 781.4 eV are assigned to $Co^{(0)}$ and CoO (Khassin *et al.*, 2012), respectively. Additionally, the characteristic satellite peak of $Co^{2+}$ is also observed at 785.9 eV (Óvári *et al.*, 2013). In addition, the XPS spectra of both fresh and spent $Co_3O_4$ catalysts are illustrated in Figure 5.2 (c) and (d). Figure 5.2 (C) shows that the Co $2p_{3/2}$ binding energies at 779.4 and 782.5 eV are assigned to $Co_3O_4$ (Biesinger *et al.*, 2012) and CoO (Khassin *et al.*, 2012), respectively. Additionally, the peak at 786.5 eV is assigned to the characteristic satellite of $Co^{2+}$ (Óvári *et al.*, 2013). For the

spent $Co_3O_4/Al_2O_3$ catalyst illustrates in Figure 5.2 (d). The Co $2p_{3/2}$ binding energy at 781.9 is assigned to CoO (Khassin *et al.*, 2012). Furthermore, the two overlapped peaks at 786.9 and 790.9 eV are assigned to the characteristic peaks of $Co^{2+}$ (Óvári *et al.*, 2013). From the results, the surfaces of both fresh $Co/Al_2O_3$ and $Co_3O_4/Al_2O_3$ do not contain only pure metallic Co and $Co_3O_4$. As depicted in Figure 5.3, the surface of fresh $Co/Al_2O_3$ consists of 93.6% Co and 6.10% CoO. Moreover, the surface of $Co_3O_4/Al_2O_3$ consists of 30.8% CoO and 69.2% $Co_3O_4$. After the catalytic testing, the surface of spent $Co/Al_2O_3$ is composed of 3.60% Co and 69.2% CoO. In addition, the surface of spent $Co_3O_4/Al_2O_3$ is composed of 100% CoO due to the reduction of $Co_3O_4$ during the reaction.

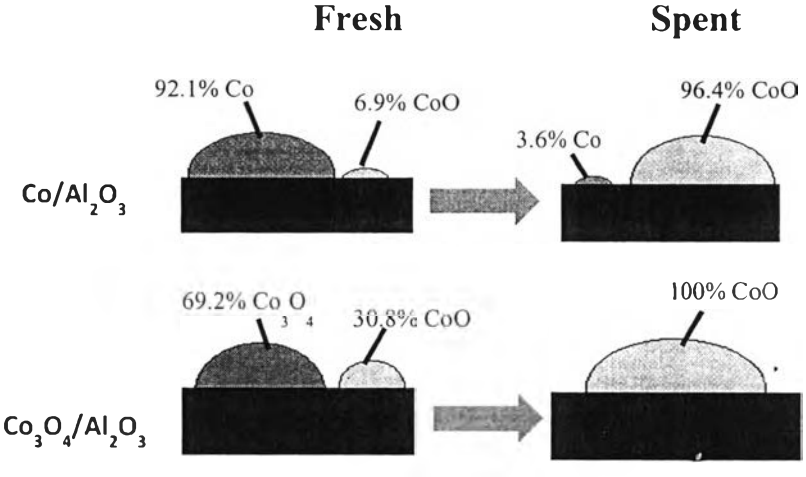


**Figure 5.3** Surface composition of cobalt-modified catalysts.

**Table 5.2** Physical properties of cobalt-modified catalysts

| Sample | Surface Area $(m^3/g)^a$ | Pore Volume $(cm^3/g)^a$ | Pore Diameter $(nm)^b$ |
|---|---|---|---|
| $Al_2O_3$ | 206.4 | 0.1792 | 49.31 |
| $Co/Al_2O_3$ | 193.2 | 0.1669 | 47.42 |
| $Co_3O_4/Al_2O_3$ | 171.8 | 0.1406 | 46.77 |

[a] determined using BET method
[b] determined using B.J.H method

Table 5.2 show the specific surface area, pore volume, and pore diameter of cobalt –promoted catalyst and parent alumina determined by using Barrette-Joyner-Halenda (BJH) method. The specific surface area and pore diameter was reduced due to the deposition of cobalt species inside the pore of alumina.

5.4.2 Catalytic Dehydration of Bio-ethanol

Bio-ethanol conversion seems to increase insignificantly, when either cobalt or cobalt oxide is individually introduced to alumina. The product obtained from ethanol dehydration can be illustrated in Figure 5.4. Moreover, the gas yield is increased; in opposition, the yield of oil and water are decreased as shown in Table 5.3. Compared to pure alumina, the gas yield is increased from 76.8 wt% to 86.8 wt%, and 82.0 wt% by using $Co/Al_2O_3$ and $Co_3O_4/Al_2O_3$, respectively. This indicates that cobalt-modified catalysts are selective to produce gaseous product. Additionally, the gas composition obtained from using alumina with cobalt and cobalt oxide promoters seem to be the same as obtained from the parent alumina. From Table 5.4, it is observed that ethylene is made dominantly from all catalysts. However, as compared to pure $Al_2O_3$, ethylene is decreased from 96.0 wt% to 64.5 wt% and 81.3 wt% by using $Co/Al_2O_3$ and $Co_3O_4/Al_2O_3$ catalysts, respectively. Additionally, the other gaseous products; that are methane, ethane, propylene, and butylene, are slightly enhanced as compare to pure $Al_2O_3$.

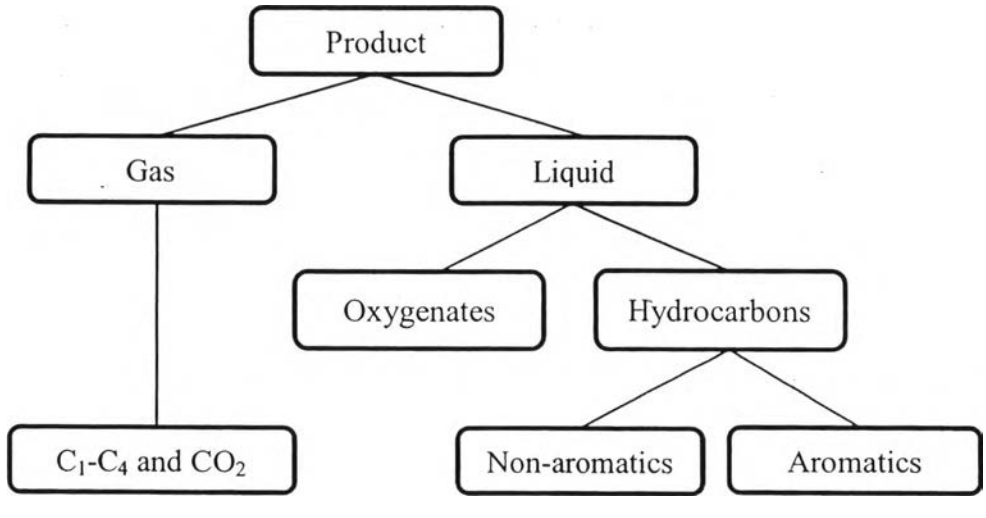


**Figure 5.4** Possible products obtained from the catalytic dehydration of bio-ethanol.

**Table 5.3** Product yields from ethanol dehydration

| Sample | % Yield | | | Conversion |
|---|---|---|---|---|
| | Oil | Water | Gas | |
| Non-catalyst | 6.2 | 11.2 | 82.6 | 99.2 |
| $Al_2O_3$ | 3.1 | 20.6 | 76.3 | 98.7 |
| $Co/Al_2O_3$ | 2.2 | 11.0 | 86.8 | 99.1 |
| $Co_3O_4/Al_2O_3$ | 2.7 | 15.3 | 82.0 | 98.9 |

The oily products are composed of two main components; that are, oxygenate compounds and hydrocarbons. The obtained oxygenate compounds and hydrocarbons using $Al_2O_3$ are accounted for 92.1 wt% and 7.9 wt% as shown in Figure 5.5, respectively. Compared to pure $Al_2O_3$, the oxygenate compounds are slightly increased from 92.1 wt% to 95.5 wt% using $Co_3O_4/Al_2O_3$. On the contrary, the hydrocarbons are slightly increased form 7.9 wt% to 11.6 wt% using $Co/Al_2O_3$. As a result, it can be noticed that using $Co/Al_2O_3$, the selectivity of hydrocarbon is increased in the conjunction with the decrease in oxygenate selectivity (Figure 5.5a)

In addition, the compositions of oil product obtained from using $Al_2O_3$ catalyst and Co-modified $Al_2O_3$ catalysts in Table 5.6 show that both $Co/Al_2O_3$ and $Co_3O_4/Al_2O_3$ give nearly the same compositions of oily product. Moreover, most of the oil products are oxygenate compounds, and the rest is hydrocarbons. The hydrocarbon product compositions obtained from using $Co/Al_2O_3$ and $Co_3O_4/Al_2O_3$ catalysts are shown in Figure 5.5b and Table 5.6. It is found that most of the hydrocarbons obtained from using $Co/Al_2O_3$ and $Co_3O_4/Al_2O_3$ are mainly distributed in $C_6$; that is, benzene. Moreover, the other hydrocarbons are present in a trace amount. Compared to parent $Al_2O_3$, benzene is significantly enhanced by using $Co/Al_2O_3$, and $C_{10}^{+}$-aromatics are slightly enhanced by using $Co_3O_4/Al_2O_3$.

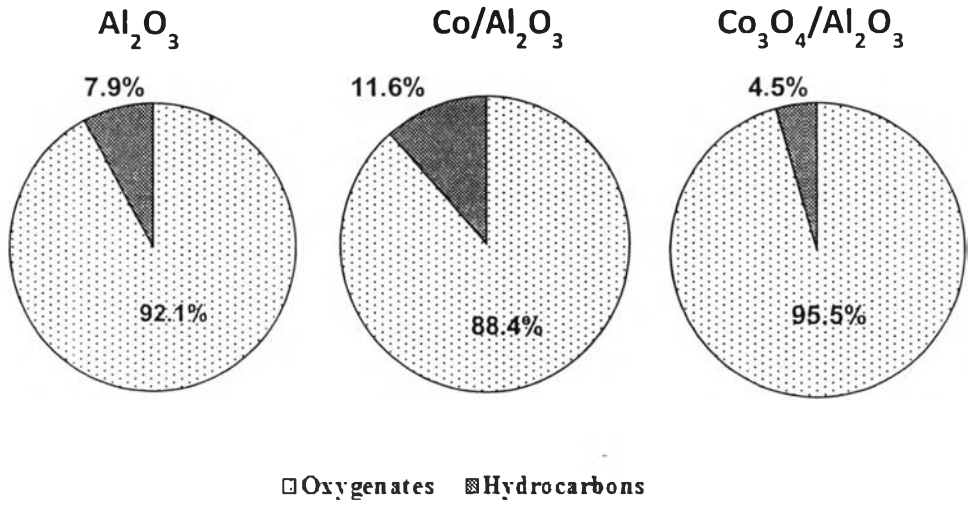


(a)

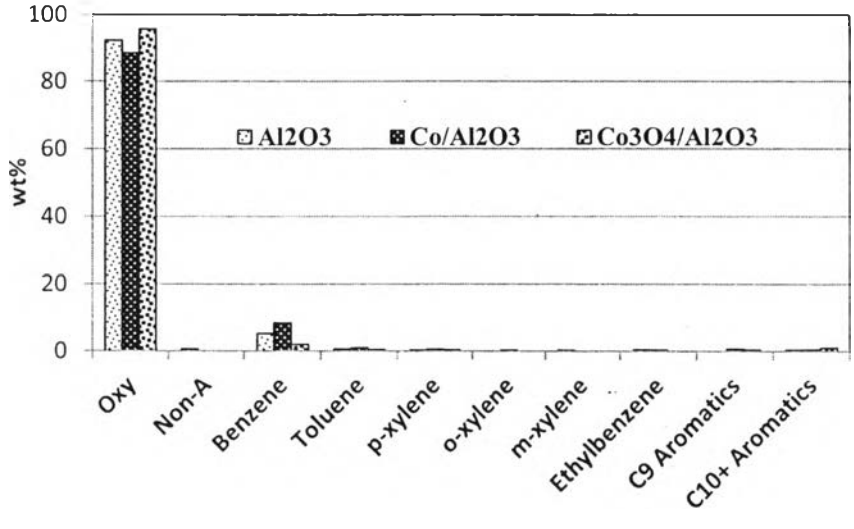


(b)

**Figure 5.5** (a) Liquid product distribution, and (b) Compositions of hydrocarbons (wt%) obtained from using Co-modified catalysts.

**Table 5.4** Gaseous product distribution obtained from bio-ethanol dehydration

| Sample | Concentration (wt%) | | | | | | | |
|---|---|---|---|---|---|---|---|---|
| | $CH_4$ | $C_2H_2$ | $C_2H_4$ | $C_3H_6$ | $C_3H_8$ | $C_4H_8$ | $C_4H_{10}$ | $CO_2$ |
| Non-catalyst | 0.0 | 99.1 | 0.6 | 0.2 | 0.0 | 0.1 | 0.0 | 0.0 |
| $Al_2O_3$ | 0.0 | 96.0 | 0.5 | 1.0 | 0.0 | 0.5 | 0.0 | 2.1 |
| $Co/Al_2O_3$ | 5.5 | 64.5 | 2.3 | 3.2 | 0.0 | 0.8 | 0.0 | 23.7 |
| $Co_3O_4/Al_2O_3$ | 3.2 | 81.3 | 1.2 | 2.2 | 0.0 | 0.7 | 0.0 | 11.2 |

Data were taken at the eight hour of time-on-stream

**Table 5.5** Oxygenates and hydrocarbons found in liquid products (wt%)

| Sample | Product Distribution (wt%) | |
|---|---|---|
| | Oxygenates | Hydrocarbons |
| Non-catalyst | 89.0 | 11.0 |
| $Al_2O_3$ | 92.1 | 7.9 |
| $Co/Al_2O_3$ | 88.4 | 11.6 |
| $Co_3O_4/Al_2O_3$ | 95.5 | 4.5 |

**Table 5.6** Compositions of hydrocarbons (wt%) obtained from using Co catalysts

| Product | Sample | | | |
|---|---|---|---|---|
| | Non-catalyst | $A_2O_3$ | $Co/Al_2O_3$ | $Co_3O_4/Al_2O_3$ |
| **Product Distribution (wt%)** | | | | |
| Oxygenates | 89.0 | 92.1 | 88.4 | 95.5 |
| Non-aromatics | 1.44 | 0.60 | 0.00 | 0.00 |
| Benzene | 4.28 | 5.20 | 8.47 | 2.08 |
| Toluene | 0.31 | 0.60 | 0.94 | 0.40 |
| p-Xylene | 0.20 | 0.20 | 0.50 | 0.30 |
| o-Xylene | 0.02 | 0.20 | 0.23 | 0.10 |
| m-Xylene | 0.03 | 0.20 | 0.03 | 0.10 |
| Ethylbenzene | 0.12 | 0.40 | 0.29 | 0.10 |
| $C_9$ aromatics | 0.10 | 0.10 | 0.65 | 0.40 |
| $C_{10}^+$-aromatics | 4.53 | 0.40 | 0.48 | 1.00 |

Data were taken at the eight hour of time-on-stream

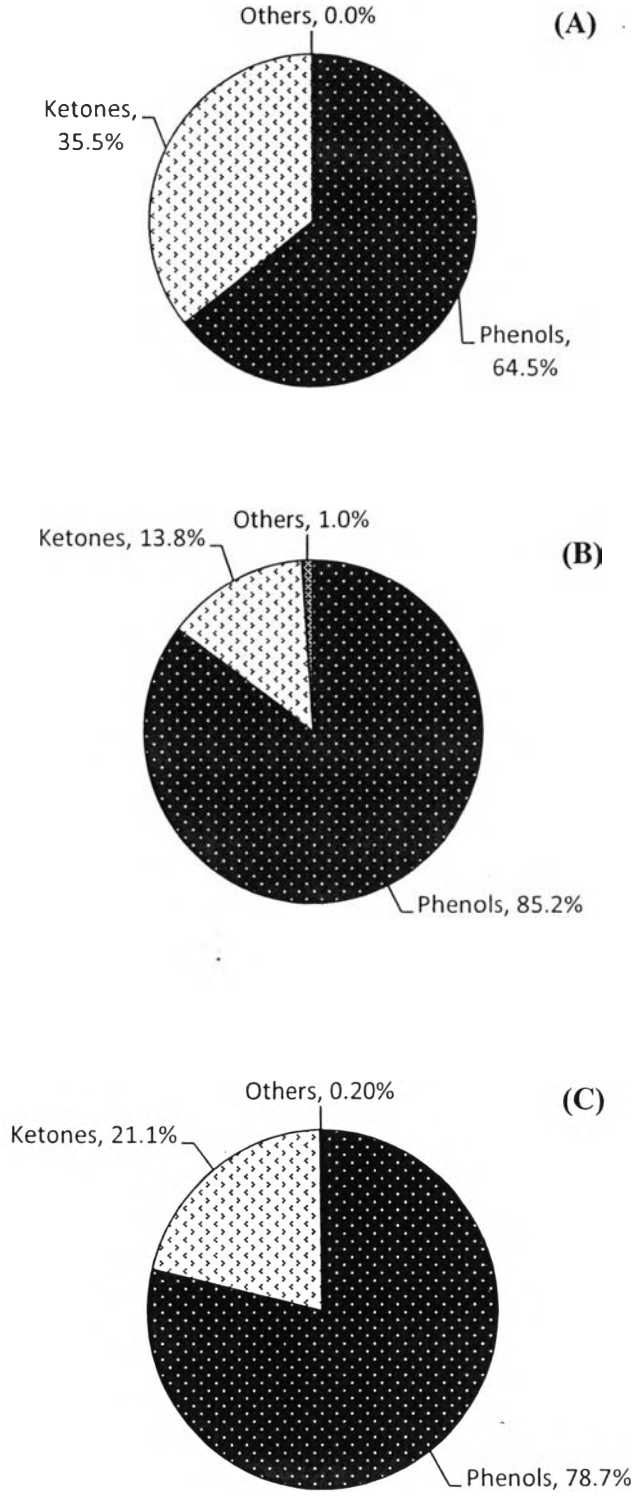


**Figure 5.6** Compositions of oxygenate compounds (wt%) found in liquid products : (A) $Al_2O_3$, (B) $Co/Al_2O_3$, and (C) $Co_3O_4/Al_2O$.

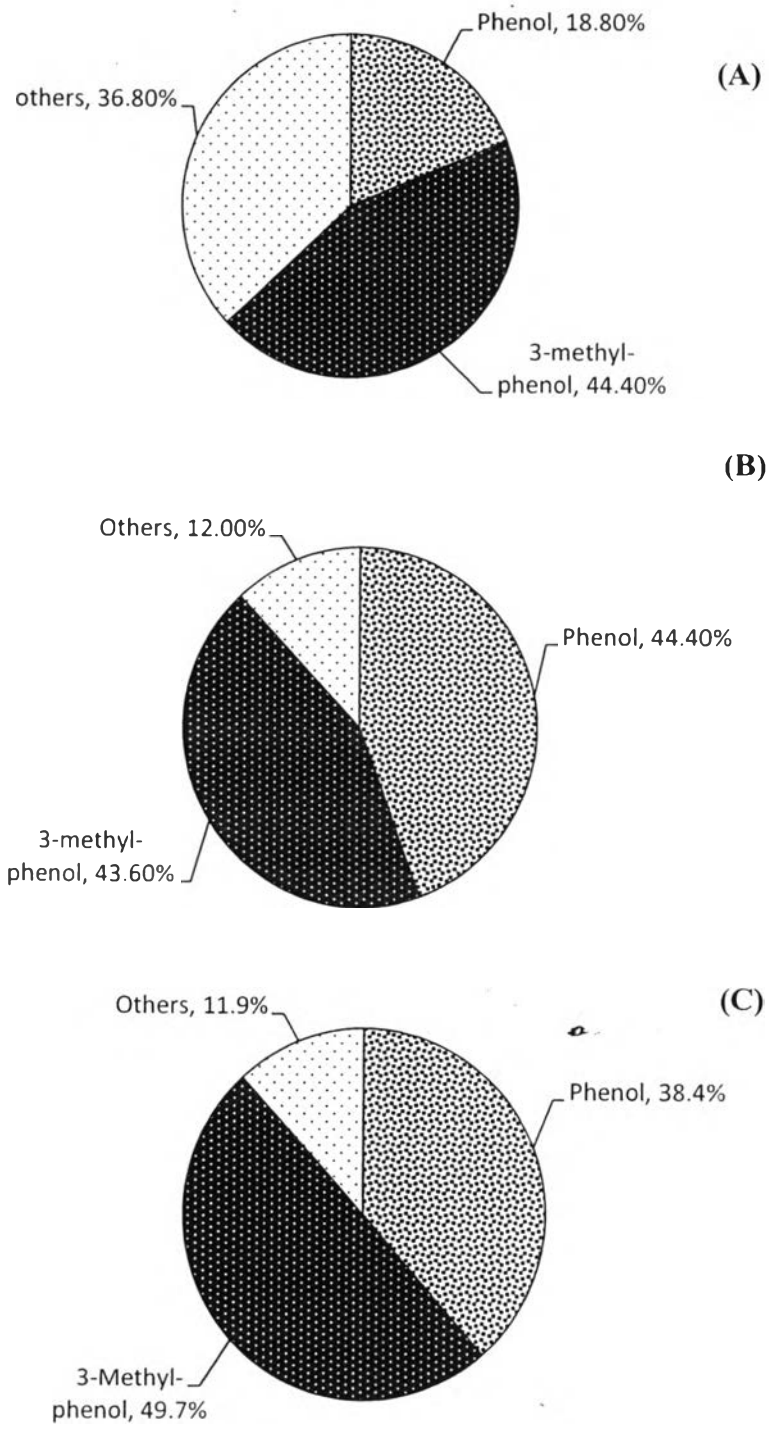


**Figure 5.7** Compositions of phenols (wt%) in oxygenate compounds : (A) $Al_2O_3$, (B) $Co/Al_2O_3$, and (C) $Co_3O_4/Al_2O_3$.

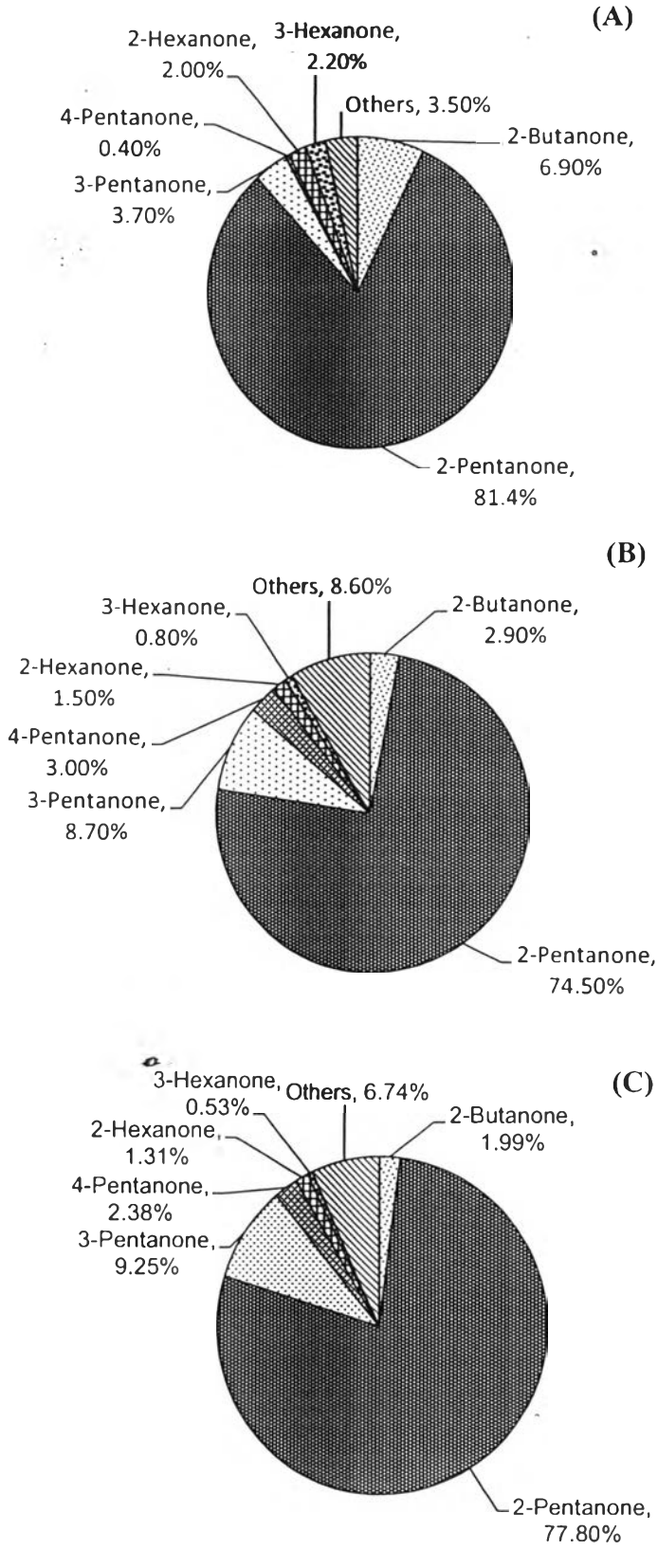


**Figure 5.8** Compositions of ketones (wt%) found in oxygenate compounds : (A) $Al_2O_3$, (B) $Co/Al_2O_3$, and (C) $Co_3O_4/Al_2O_3$.

5.4.3 Oxygenate Compounds Production

The composition of oxygenate compounds obtained from the catalytic dehydration of bio-ethanol are shown in Figure 5.6. It is found that the oxygenate compounds are composed of two main components; that are, phenol and ketone compounds. Additionally, the others are a trace of ethers. Compared to parent alumina, phenol compounds are significantly increased from 64.5 wt% to 85.2 wt% and 78.7 wt% by using $Co/Al_2O_3$ and $Co_3O_4/Al_2O_3$, respectively. However, ketone compounds are slightly decreased from 35.5 wt% to 13.5 wt%, and 21.1 wt% using cobalt-modified catalysts. As a result, it can be noticed that both $Co/Al_2O_3$ and $Co_3O_4/Al_2O_3$ give nearly the same compositions of oxygenate compounds; that are, phenols and ketones. This means that both cobalt-modified catalysts promote the same pathways of oxygenate compounds formation.

Figure 5.6 shows that phenol compounds are found as main component in oxygenate compounds obtained from cobalt-modified catalysts. Among phenol compounds, phenol is a high value solvent and widely used in many applications. In general, phenol is widely used as a precursor for producing polymer, like polycarbonate and nylons. Moreover, it also can be used as raw material for producing some kind of pharmaceutical drugs. As compared to unmodified alumina in Figure 5.7, phenol selectivity is significantly enhanced from 18.8 wt% to 44.4 wt% and 38.4 wt% by using $Co/Al_2O_3$ and $Co_3O_4/Al_2O_3$, respectively. Moreover, phenol selectivity can be ranked as follows: $Co/Al_2O_3 > Co_3O_4/Al_2O_3 > Al_2O_3$.

In addition, ketone compounds are found as the component group with the second highest amount in oxygenate compounds using Co-modified catalysts. From Figure 5.8, among ketone compounds, 2-pentanone, a high valuable solvent widely used in many applications, is found as the major component. As a result, 2-pentanone selectivity is slightly decreased from 81.4 wt% to 74.5 wt% and 77.8 wt% by using $Co/Al_2O_3$ and $Co_3O_4/Al_2O_3$, respectively. Furthermore, 2-pentanone selectivity can be ranked as follows: $Al_2O_3 > Co_3O_4/Al_2O_3 > Co/Al_2O_3$.

5.4.4 Effect of Oxidation State of Co

In order to investigate the effect of oxidation state of Co on product distribution, the cobalt-modified catalysts with two oxidation states of cobalt promoters were examined in the catalytic dehydration of bio-ethanol, and compared. Based on the results, the distribution of oxygenate compounds and hydrocarbons play an important role on determination of the promoter effect. From Table 5.7, it can be noticed that different oxidation states of cobalt promoters might promote different pathways of ethanol transformation, and give different product distribution. Using oxidation state of zero of cobalt as promoter; that is $Co/Al_2O_3$ catalyst, the hydrocarbons is slightly enhanced from 7.9 wt% to 11.6 wt%, but oxygenate compounds are slightly suppressed as compared to the un-promoted catalyst. This means that $Co/Al_2O_3$ catalyst prefers promoting ethanol dehydration to ethanol dehydrogenation, resulting in the increases in hydrocarbons in oil products. However, the use of oxidation state of 2.67+; that is $Co_3O_4/Al_2O_3$ catalyst, promotes different pathways of ethanol transformation. The result shows that the selectivity of oxygenate compounds are slightly increased from 92.1 wt% to 95.5 wt%, while the selectivity of hydrocarbons are suppressed. This implies that $Co_3O_4/Al_2O_3$ catalyst prefers promoting ethanol dehydrogenation to dehydration, resulting in the increasing of oxygenate compounds. Furthermore, it can be concluded that different oxidation state of cobalt promotes different pathways of ethanol transformation, meaning that with the use of $Co_3O_4/Al_2O_3$, the reaction is driven to Pathway A in Figure 5.7, resulting in the increasing of oxygenate compounds. On the other hand, the use of $Co/Al_2O_3$ catalyst drives the reactions to Pathway B in Figure 5.9

**Table 5.7** Liquid product distribution from using cobalt catalyst

| Catalyst | Product Distribution (wt%) | |
|---|---|---|
| | Oxygenates | Hydrocarbons |
| $Al_2O_3$ | 92.1 | 7.9 |
| $Co/Al_2O_3$ | 88.4 | 11.6 |
| $Co_3O_4/Al_2O_3$ | 95.5 | 4.5 |

Furthermore, the result of GC×GC-TOF/MS indicates that there is no non-aromatics formation; in opposition, benzene is only found as a primary hydrocarbon obtained from using the $Co/Al_2O_3$ catalyst. This indicates that $Co/Al_2O_3$ catalyst directly promotes the formation of hydrocarbons through ethylene aromatization, meaning that ethylene that is decreased in the gaseous product might directly transform to benzene via aromatization reaction as illustrated in Figure 5.10. Additionally, the oxygenate compounds are generally produced through ethanol dehydrogenation over a metal oxide catalyst (Tuti and Pepe, 2008) due to metal oxides that contain oxygen adatoms, leading to the formation of anion vacancies on metal oxide surface once used by the reaction (de Lima *et al.*, 2009). This oxygen vacancy is able to abstract hydrogen atom at hydroxyl group, resulting in dehydrogenation reaction. After ethanol undergoes dehydrogenation, aldehyde is formed as a primary oxygenate compounds. Moreover, aldehyde can undergo condensation to form aldor species, which are found as important species that convert to other oxygenate compounds. As shown in Figure 5.11, aldor species can thermodynamically transform to acetone, and yield formaldehyde as a co-product. Likewise, aldehyde and acetone can react to one another via aldehyde-acetone condensation and hydrogenation, leading to 2-pentanone formation and yielding water as a by-product. Furthermore, phenol might be formed by decarbonylation of keto intermediate, and then reacts to another alcohol molecule, resulting in phenol formation.

Additionally, the formation of oxygenate compounds can be occurred by ethanol adsorbed at the vacancy of metal oxide surface, leading to ethoxy species formation. Zafeiratos *et al.*, (2010) found that cobalt oxide could be reduced by methanol, forming carbon dioxide and water as by-product. This implies that $Co_3O_4$ is reduced by ethanol during the catalytic testing, forming ethoxy species that adsorbed on the metal oxide surface. The carbon dioxide formation in the gaseous products supports the explanation. In addition, although $Co/Al_2O_3$ catalyst exhibits the increases in hydrocarbons, but the oxygenate compounds still a main product in oil, indicating that the formation oxygenate compounds is also governed by $Al_2O_3$ support because $Al_2O_3$ is also classified as one kind of metal oxide catalyst

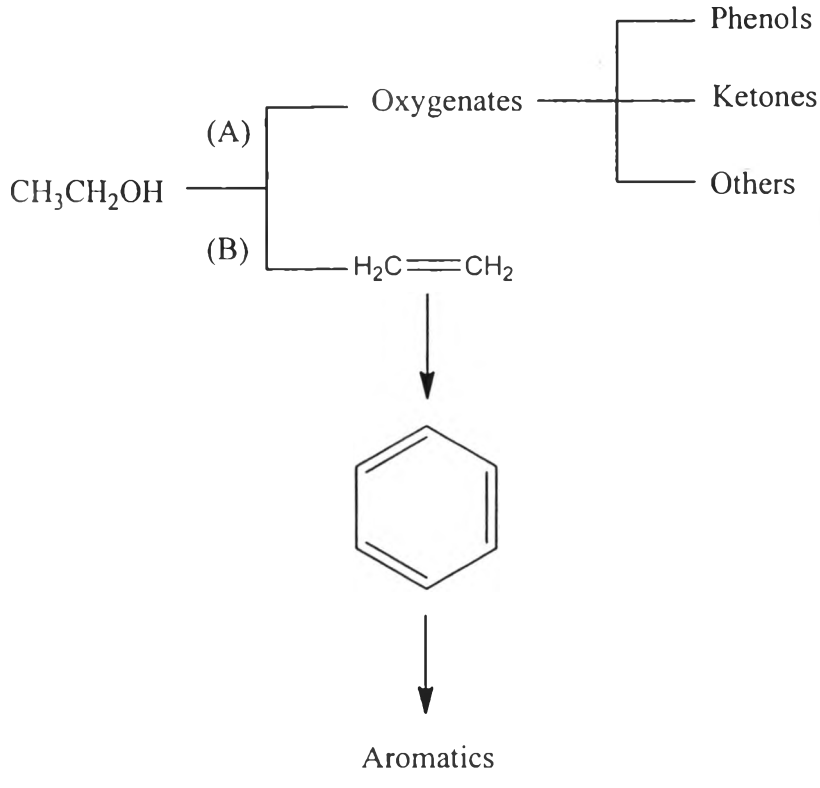


**Figure 5.9** Ethanol transformation pathways using Co-modified catalysts: (A) Ethanol dehydration, and (B) Ethanol dehydrogenation.

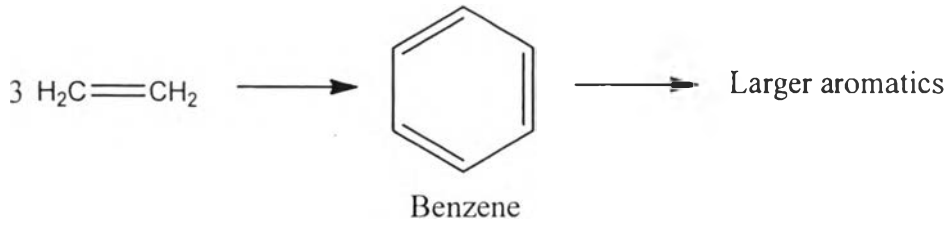


**Figure 5.10** Aromatic formation from ethylene (Bargin *et al.*, 1996).

## 5.5 Conclusions

Cobalt promoters with different oxidation states were investigated in the catalytic dehydration of bio-ethanol, aiming to investigate the effect of oxidation state on product distribution. From the results, it was revealed that different oxidation states of cobalt promoter promoted different reaction pathways, and more selectively produced different products. Metallic Co-promoted alumina favored to promote hydrocarbon products via ethanol dehydration as the outstanding reaction pathway. Moreover, the hydrocarbons were composed of benzene, toluene, mixed-xylenes, $C_9$, and $C_{10}^+$-aromatics without non-aromatics formation. On the contrary, cobalt oxide-promoted alumina favored to promote different outstanding reaction; that is, ethanol dehydrogenation. The oxygenate compounds were composed of phenol and ketone compounds. Furthermore, XPS analysis indicated that metallic Co was partially oxidized to CoO, but $Co_3O_4$ was totally reduced to CoO after the catalytic testing. Therefore, the ease of reducibility can be ranked in the order of $Co_3O_4$>CoO.

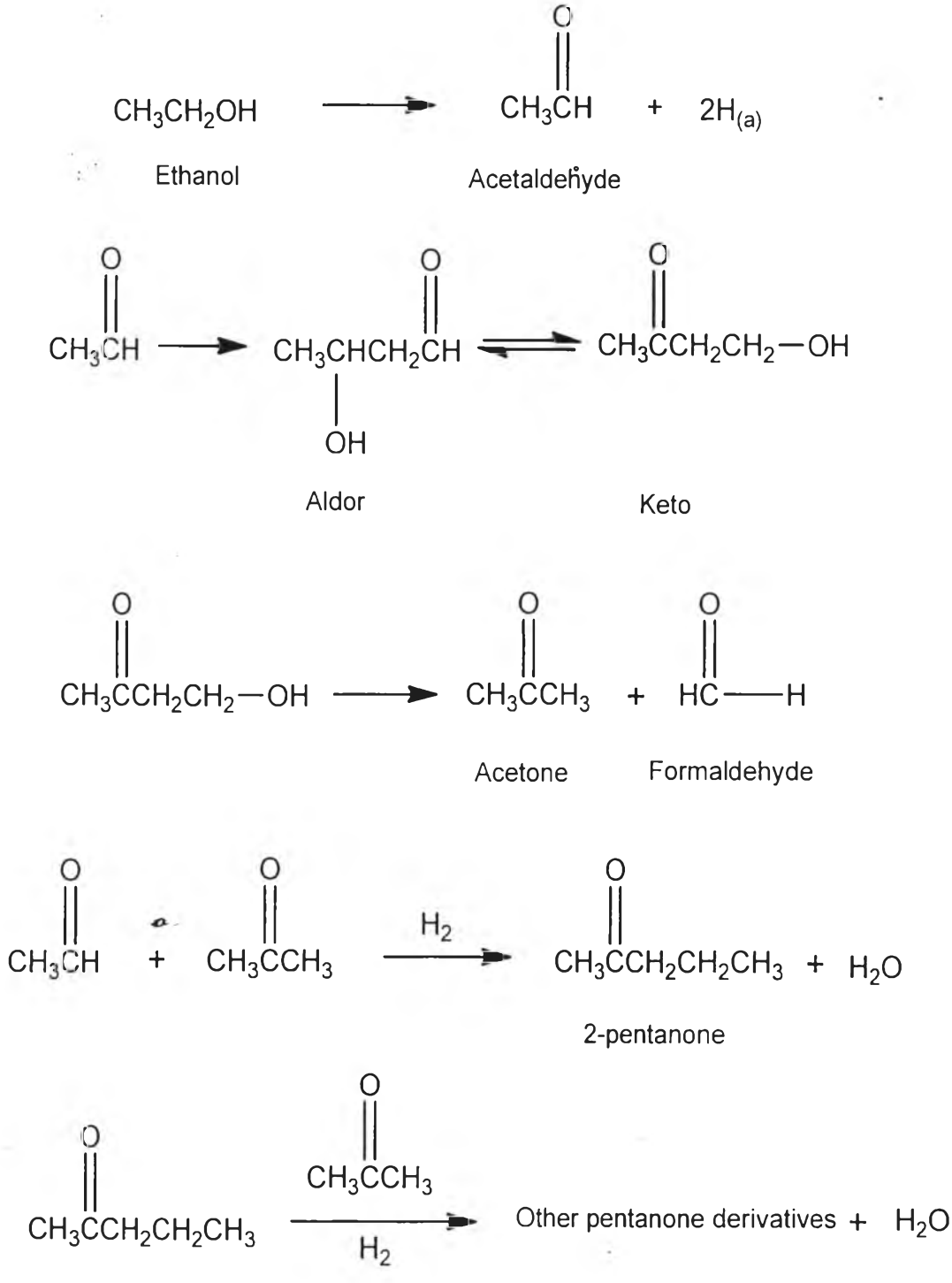


**Figure 5.11** Reaction pathways of ethanol to pentanones (He *et al.*, 2005).

## 5.6 References

Batista, M. S., Santos, Rudye K. S., Assaf, Elisabete M., Assaf, José M., Ticianelli, Edson A. 2003, Characterization of the activity and stability of supported cobalt catalysts for the steam reforming of ethanol, Journal of Power Sources 124(1), 99-103.

Biesinger, M. C., Payne, B. P., Grosvenor, A. P., Lau, L. W. M., Gerson, A. R., Smart, R. St C. ,2011, Resolving surface chemical states in XPS analysis of first row transition metals, oxides and hydroxides: Cr, Mn, Fe, Co and Ni, Applied Surface Science 257(7), 2717-2730.

Bechara, R., Balloy, D., and Vanhove, D. (2001) Catalytic properties of $Co/Al_2O_3$ system for hydrocarbon synthesis. Applied Catalysis A: General, 207(1–2), 343-353.

Bragin, O. V., Preobrazhenskii, A. V., Liberman, A. L. (1974) Catalytic cyclotrimerization of ethylene to benzene. Bulletin of the Academy of Sciences of the USSR, Division of chemical science, 23(12), 2654-2659.

Cant, N.W., Liu, I.O.Y., and Scott, J.A. (2013) Ethylene oligomerisation over $Co/SiO_2$ in the presence of trace carbon monoxide: The Eidus reaction revisited. Catalysis Today, 215, 267-275.

Chinniyomphanich U., Jitkarnka S., (2014) Metallic Sn- and $SnO_2$-doped SAPO-34 as model catalysis for investigating the effect of oxidation states on bio-ethanol dehydration product, Chemical Engineering Transaction, 39, 937-942.

de Lima, S.M., da Silva, A.M., da Costa, L.O.O., Graham, U.M., Jacobs, G., Davis, B.H., Mattos, L.V., and Noronha, F.B. (2009). Study of catalyst deactivation and reaction mechanism of steam reforming, partial oxidation, and oxidative steam reforming of ethanol over $Co/CeO_2$ catalyst. Journal of Catalysis, 268(2), 268-281.

He, D., Ding, Y., Chen, W., Lu, Y., Luo, H. (2005) One-step synthesis of 2-pentanone from ethanol over K-Pd/MnOx-$ZrO_2$-ZnO catalyst. Journal of Molecular Catalysis A: Chemical 226(1), 89-92.

Iglesia, E. (1997) Design, synthesis, and use of cobalt-based Fischer-Tropsch synthesis catalysts. Applied Catalysis A: General, 161 (1–2), 59-78.

Kagyrmanova, A.P., Chumachenko, V.A., Korotkikh, V.N., Kashkin, V.N. and Noskov, A.S. (2011) Catalytic dehydration of bioethanol to ethylene: Pilot-scale studies and process simulation. Chemical Engineering Journal, 176–177, 188-194.

Khassin, A. A., Yurieva, T. M., Kaichev, V. V., Bukhtiyarov, V. I., Budneva, A. A., Paukshtis, E. A., Parmon, V. N. (2001) Metal–support interactions in cobalt-aluminum co-precipitated catalysts: XPS and CO adsorption studies. Journal of Molecular Catalysis A, Chemical 175(1–2), 189-204.

Liu, C., Li, J., Zhang, Y., Chen, S., Zhu, J., Liew, K. (2012) Fischer–Tropsch synthesis over cobalt catalysts supported on nanostructured alumina with various morphologies. Journal of Molecular Catalysis A: Chemical, 363–364, 335-342.

Óvári, L., Krick C., S., Lykhach, Y., Libuda, J., Erdőhelyi, A., Papp, C., Kiss, J., Steinrück, H. P. (2013) Near ambient pressure XPS investigation of the interaction of ethanol with $Co/CeO_2$. Journal of Catalysis, 307, 132-139.

Ozkan, U.S., Kueller, R.F., and Moctezuma, E. (1990) Methanol oxidation over nonprecious transition metal oxide catalysts. Industrial & Engineering Chemistry Research, 29(7), 1136-1142.

Takahara, I., Saito, M., Matsuhashi, H., Inaba, M., Murata, K. (2007) Increase in the number of acid sites of a H-ZSM5 zeolite during the dehydration of ethanol. Catalysis Letters, 113(3-4), 82-85.

Tuti, S. and Pepe, F. (2008) On the Catalytic Activity of Cobalt Oxide for the Steam Reforming of Ethanol. Catalysis Letters, 122(1-2), 196-203.

Wang, L., Hisada, Y., Koike, M., Li, D., Watanabe, H., Nakagawa, Y., Tomishige, K. (2012) Catalyst property of Co–Fe alloy particles in the steam reforming of biomass tar and toluene. Applied Catalysis B: Environmental, 121–122, 95-104.

Zafeiratos, S., Dintzer, T., Teschner, D., Blume, R., Hävecker, M., Knop-Gericke, A., Schlögl, R. (2010) Methanol oxidation over model cobalt catalysts: Influence of the cobalt oxidation state on the reactivity. Journal of Catalysis, 269(2), 309-317.

Zhang, X., Wang, R., Yang, X. and Zhang, F. (2008) Comparison of four catalysts in the catalytic dehydration of ethanol to ethylene. Microporous and Mesoporous Materials, 116 (1–3), 210-215.